Robotica (2006) volume 24, pp. 315–324. © 2005 Cambridge University Press
doi:10.1017/S0263574705002195 Printed in the United Kingdom

Modeling and simulation of swarms for collecting objects

Yangmin Li* and Xin Chen

Department of Electromechanical Engineering, Faculty of Science and Technology, University of Macau, Av.Padre Tomás Pereira S.J., Taipa, Macau SAR (P. R. China)

(Received in Final Form: July 5, 2005, first published online 31 October 2005)

SUMMARY

A mathematic model is established to describe a swarm with multi-behavior. Regarding a swarm designed for cooperative task, we propose a model which includes a macroscopic model and a individual-based model. The macroscopic framework model describes global dynamics of swarms, which is normally expressed by dynamical populations' densities with different behaviors, while the individual-based framework model describes a individual agent's trajectory. Based on these models, we prove that all objects can be collected to the "home" area under conditions of individual agents subject to sensor constraints.

KEYWORDS: Swarm intelligence; Macroscopic model; Individual-based model; Markov process; Non-smooth system.

I. INTRODUCTION

Swarming behavior can usually be observed in fish, birds, bees, and herds of mammals for avoiding predators to increase the survival rate or enhancing the hunting successful rate through collaborations.[1,2] The performance of swarms has characteristics of self-organization since individuals in swarms interact with each other or with their environment in order to achieve a group goal. With properties of self-organization, stigmergy, and decentralization, a swarm paradigm is more efficient, adaptive, and robust than the traditional *AI* paradigm that is based on deliberative agents and central control method.

The main difficulty in studying swarms is to understand the effect of individual behavior on the collective behavior of the entire system. Swarms can be described by two kinds of models: macroscopic model and microscopic model. The macroscopic model can be described by the discrete time or continuous time Markov process.[3,4] If a macroscopic model just describes temporal variety of the system, a nonspatial approach can be used. Another kind of Eulerian framework describes the swarm dynamics via a continuum model of the flux, namely concentration or population density.[5,6] Although a macroscopic model can reduce the complexities in description of swarms, it cannot describe the behaviors of individuals in details. In contrast, a microscopic model or individual-based (Lagrangian) framework[7] is good at describing individual motions and interactions, which is preferable for analyzing on a task whose main purpose is to describe the relationship of individuals' motions in terms of formation and aggregation.[8–10] Therefore many research works can be found on the stability of swarms based on individual-based models.[11] An individual-based model has another advantage of facilitating the design of individual control strategy using traditional control techniques. In the microscopic model, a social potential field is widely used for quantitatively describing the interactions among individuals. The motion of individuals is controlled by the resultant artificial forces imposed by other robots or the environment.[7,12–14] In fact, most individual-based models are designed for the formation or aggregation task, with only simple behavior.[15–18] But for other tasks, including multiple behaviors or agents, it is difficult to describe behaviors or roles by using individual-based model. Hence the macroscopic model can be exploited to describe the swarming dynamics in terms of population density, which is suitable for describing transformation of behaviors, while an individual-based model is preferable at description of individual motion.

This paper proposes a design of swarms for cooperative collecting task with a detailed mathematical description. The whole system model is established by an integration of both macroscopic model and individual-based model. The macroscopic framework describes the dynamics of statistical distribution of swarms, while the motions of individuals will be described by the individual-based framework. It has been proved that even if members of the swarms subject to sensing constraints and avoiding collisions, they still can move all objects to the desired area.

The rest of the paper is organized as follows: A general mathematical model for swarms is set up in Section II. In Section III, based on two transportation velocity strategies, swarm performance is discussed. Section IV presents some conclusions on the swarm design.

II. MATHEMATICAL MODELING

The goal of swarms for cooperative collecting task is to collect all objects scattered randomly within the arena to the "home" area. To simplify the analysis, we assume that the "home" area is static. Generally an agent's motion in collecting task can be expressed briefly as follows: When a member of swarms searching within an arena encounters an object, it will decide whether to attach itself to the object

* Corresponding author. E-mail: ymli@umac.mo|ya27407@umac.mo

or not. If it decides to attach to the object, there are two situations: 1) If there are no other agents attaching to the object, it will wait for help. If it fails to wait for others' help within a certain period, the agent will abandon the attachment; 2) If there is another agent attaching to the object, the agent will work with its partner to move the object to the "home" area. During the process of transportation, they may give up transportation, which will be explained later, for the abandonment strategy. Obviously two agents are needed to move a single object.

To illustrate the model, some assumptions and definitions are introduced as follows:

Assumptions:

1) There are M identical objects whose positions are represented by $\vec{D}_i (i = 1, \ldots M)$;
2) There are N agents, in other words the size of swarm is N;
3) All individuals have identical perceiving ability indicated by α, which represents the probability of a robot encountering an object at any time, whose value can be derived by stochastic techniques, such as Monte-Carlo method.

Definitions:

1) The states of object i:
   i) S_{i1}: No agents attaching to object i;
   ii) S_{i2}: One agent attaching to object i. It is also called the state waiting for cooperation;
   iii) S_{i3}: Two agents attaching to object i. Since an object in the state has opportunity to be moved, it is also called as the transportation state.

They form an event set in terms of $\{S_{i1}, S_{i2}, S_{i3}\}$, in which all events are mutually exclusive;

2) The states of the swarm:
   i) N_S: The number of agents searching within the arena;
   ii) N_W: The number of agents waiting for help;
   iii) N_T: The number of agents transporting objects.

Obviously, there exists a constraint: $N_S + N_W + N_T = N$;

3) Attachment rate f_{i1}, which represents a probability at which an individual decides to catch the object or not. It is somewhat like a degree describing how interested agents feel to attach to the objects that they encounter;
4) Abandonment rate f_{i2}, which represents a probability at which object i in the transportation state is abandoned by the two agents attaching to it. Such abandonment rate can be regarded as a kind of boredom felt by agents to move object i;
5) Waiting period of τ. When an agent is attaching to an object alone, it will wait for cooperation for a constant period of τ. If no other agents attach to the object during period of τ, the agent will abandon attachment;
6) The velocity of transportation $\bar{v}$. It is the speed at which two agents move an object together, or moving speed of an object in the transportation state.

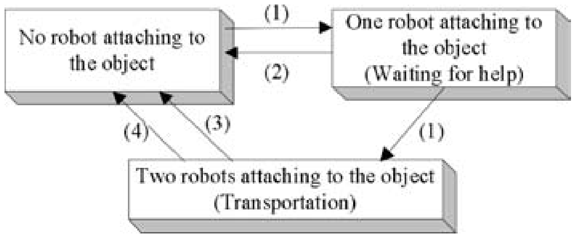

Fig. 1. The object's states diagram.

The process obeys the properties of state-discrete and parameter-continuous Markov process, which includes three kinds of dynamics shown in the following subsections.

II.1. Dynamics of objects' states

The dynamics of object's states will reflect the Markov properties of the system. Figure 1 shows the states diagram of objects dynamics. The tabs represent four reasons for state transitions: (1) An agent attaches itself to an object; (2) An agent gives up waiting for help; (3) Agents abandon transportation as a result of boredom; (4) Object is blocked while transporting.

For object i, $X_i = [X_{i1} \ \ X_{i2} \ \ X_{i3}]^T$ is defined as the absolute states' distribution for the event set $\{S_{i1}, S_{i2}, S_{i3}\}$. Obviously, there exists a distribution constraint: $X_{i1} + X_{i2} + X_{i3} = 1$. The dynamics of distribution can be expressed as

$$X_i'(t) = \lim_{\Delta t \to 0} \frac{X_i(t + \Delta t) - X_i(t)}{\Delta t} = A_i X_i(t), \qquad (1)$$

where A_i is the density matrix of transition probability in the form of

$$A_i = \{a_{ijk}\} = \begin{bmatrix} -\alpha N_S f_{i1} & \alpha N_{S(-\tau)} \Gamma_i & f_{i2} \\ \alpha N_S f_{i1} & -(\alpha N_{S(-\tau)} \Gamma_i + \alpha N_S f_{i1}) & 0 \\ 0 & \alpha N_S f_{i1} & -f_{i2} \end{bmatrix} \qquad (2)$$

The entries of A_i can be divided into three kinds: 1) Describing attachment, such as $a_{i21} = \alpha N_S f_{i1}$; 2) Describing abandonment, such as $a_{i13} = f_{i2}$; 3) Describing waiting for help, such as $a_{i12} = \alpha N_{S(-\tau)} \Gamma_i$, which describes the probability at which object i in state S_{i2} is abandoned by the only agent. $N_{S(-\tau)}$ denotes $N_S(t - \tau)$. $\Gamma_i(\tau)$ is the probability of no agents coming to help during time interval $[t - \tau, \ t]$, which can be computed by

$$\begin{aligned} \Gamma_i(\tau) &= \lim_{\Delta t \to 0} \prod_{i=1}^{\tau/\Delta t} [1 - \alpha N_S(t - \tau + i\Delta t) \\ &\quad \times f_{i1}(t - \tau + i\Delta t)]\theta(t - \tau) \\ &= \exp\left[-\alpha f_{i1}(t - \tau) \int_{t-\tau}^{t} N_S(s)\, ds\right] \theta(t - \tau) \qquad (3) \end{aligned}$$

where $\theta(t - \tau)$ is a step function to ensure that $\forall s \notin [t - \tau, t]$ and $\Gamma_i(\tau) = 0$, while during period $s \in [t - \tau, t]$, $f_{i1}(s) \equiv f_{i1}(t - \tau)$.

II.2. Dynamics of agents' states

The dynamics of agents' states describes the change of number of agents in different behaviors, including searching, waiting for help, and moving objects. We take dynamics of N_S, the number of agents in searching state, as an example. According to object states, a stochastic variable $\varphi(S_i(t))$ for object i is defined as

$$\varphi(S_i(t)) = \begin{cases} 0, & S_i(t) = S_{i1} \\ 1, & S_i(t) = S_{i2} \\ 2, & S_i(t) = S_{i3} \end{cases}. \tag{4}$$

Then N_S can be expressed as $N_S(t) = N - \sum_{i=1}^{M} \varphi(S_i(t))$. Consequently, the expectance of N_S is

$$\begin{aligned} E(N_S(t)) &= N - \sum_{i=1}^{M} E(\varphi(S_i(t))) \\ &= N - \sum_{i=1}^{M} X_{i2}(t) - \sum_{i=1}^{M} 2 \cdot X_{i3}(t) \end{aligned} \tag{5}$$

Differentiating $E(N_S(t))$, we can obtain the expectant dynamics of N_S by

$$\begin{aligned} E\left(\frac{dN_S}{dt}\right) = \sum_{i=1}^{M} \Big(&-\alpha N_S f_{i1} X_{i1} - \alpha N_S f_{i1} X_{i2} \\ &+ \alpha N_{s(-\tau)} \Gamma X_{i2(-\tau)} + 2 \cdot f_{i2} X_{i3} \Big) \end{aligned} \tag{6}$$

where $X_{i2(-\tau)}$ denotes $X_{i2}(t-\tau)$. Similarly we can obtain the dynamics of other two states N_W and N_T in terms of (13) and (14).

II.3. Moving speed of objects

If an object is regarded as a kind of particle, according to Definition 6), the expectant moving speed of object i is

$$\begin{aligned} E\left(\frac{d\vec{D}_i}{dt}\right) &= \lim_{\Delta t \to 0} E\left(\frac{\vec{D}_i(t+\Delta t) S_i(t+\Delta t) - \vec{D}_i(t) S_i(t)}{\Delta t}\right) \\ &= \bar{v} \cdot X_{i3}(t) \end{aligned} \tag{7}$$

The transportation velocity $\bar{v}$ plays a very important role in swarm design, which determines the way that how objects are transported to the home area. In the following section, the swarm performance will be analyzed according to different strategies of the transportation velocity.

II.4. The general mathematical model of the swarm

The dynamic equations of the expectant system can be expressed as follows with the denotations of expectation omitted for simplifications.

$$\frac{dX_{i1}}{dt} = -\alpha N_S f_{i1} X_{i1} + \alpha N_{s(-\tau)} \Gamma_i X_{i2(-\tau)} + f_{i2} X_{i3} \tag{8}$$

$$\frac{dX_{i2}}{dt} = \alpha N_S f_{i1} X_{i1} - \alpha N_{S(-\tau)} \Gamma_i X_{i2(-\tau)} - \alpha N_S f_{i1} X_{i2} \tag{9}$$

$$\frac{dX_{i3}}{dt} = \alpha N_S f_{i1} X_{i2} - f_{i2} X_{i3} \tag{10}$$

$$\frac{d\vec{D}_i}{dt} = \bar{v}_i \cdot X_{i3} \tag{11}$$

$$\begin{aligned} \frac{dN_S}{dt} = \sum_{i=1}^{M} \Big(&-\alpha N_S f_{i1} X_{i1} - \alpha N_S f_{i1} X_{i2} \\ &+ \alpha N_{s(-\tau)} \Gamma_i X_{i2(-\tau)} + 2 \cdot f_{i2} X_{i3} \Big) \end{aligned} \tag{12}$$

$$\frac{dN_W}{dt} = \sum_{i=1}^{M} \left(\alpha N_S f_{i1} X_{i1} - \alpha N_S f_{i1} X_{i2} - \alpha N_{s(-\tau)} \Gamma_i X_{i2(-\tau)} \right) \tag{13}$$

$$\frac{dN_T}{dt} = \sum_{i=1}^{M} (2 \cdot \alpha N_S f_{i1} X_{i2} - 2 \cdot f_{i2} X_{i3}) \tag{14}$$

where $i = 1, 2, \cdots, M$.

Obviously, $\sum_{j=1}^{3} \frac{dX_{ij}}{dt} = 0$ and $\frac{dN_S}{dt} + \frac{dN_W}{dt} + \frac{dN_T}{dt} = 0$. Because the transition density matrix A_i is related to the position of object i, the collection process is a non-homogeneous Markov process.

III. PERFORMANCE ANALYSIS

We will concentrate on the analysis for the expectant traces of the objects.

III.1. Markov properties of dynamics of object states

For object i, states set $\{S_{i1}, \ S_{i2}, \ S_{i3}\}$ includes a single irreducible subset of states. If the position of object i is fixed, there exists a unique stationary distribution, denoted as $\{\pi_{i1}, \ \pi_{i2}, \ \pi_{i3}\}$, which is expressed as

$$\pi_{i1} = \frac{f_{i1} f_{i2} + f_{i2} \Gamma_i}{\alpha N_S f_{i1}^2 + 2 f_{i1} f_{i2} + f_{i2} \Gamma_i} \tag{15}$$

$$\pi_{i2} = \frac{f_{i1} f_{i2}}{\alpha N_S f_{i1}^2 + 2 f_{i1} f_{i2} + f_{i2} \Gamma_i} \tag{16}$$

$$\pi_{i3} = \frac{\alpha N_S f_{i1}^2}{\alpha N_S f_{i1}^2 + 2 f_{i1} f_{i2} + f_{i2} \Gamma_i} \tag{17}$$

Here two conclusions are useful in following proofs of stability of the swarm:

1) If $f_{i1} \neq 0$, then $\pi_{i3} \neq 0$. That means if an object has an opportunity to be picked up by agents, it must have opportunity to change into the transportation state.
2) $\lim_{f_{i1} \to 0, f_{i2} \to 1} \pi_{i3} = 0$. That means if agents have little interests in moving objects, objects have little opportunities to change into the transportation state.

III.2. The model without sensor constraints

In this subsection, we analyze the performance of the system if agents have infinite perceiving ability to perceive all objects' positions for collision avoidance. It is assumed that

https://doi.org/10.1017/S0263574705002195 Published online by Cambridge University Press

the attachment and abandonment rate obey the following principles:

$$\lim_{\|\vec{D}_i - H\|\to 0} f_{i1}(\|\vec{D}_i - H\|) = 0, \quad \lim_{\|\vec{D}_i - H\|\to \infty} f_{i1}(\|\vec{D}_i - H\|) = 1 \tag{18}$$

$$\lim_{\|\vec{D}_i - H\|\to 0} f_{i2}(\|\vec{D}_i - H\|) = 1, \quad \lim_{\|\vec{D}_i - H\|\to \infty} f_{i2}(\|\vec{D}_i - H\|) = 0 \tag{19}$$

where H is the center of the "home" area.

III.2.1. Transportation velocity based on artificial potential field. We suppose that there exists an artificial potential field, so that each object in the field has a potential energy denoted by E. The potential profile includes attraction profile $\sigma_i(\vec{D}_i)$, which makes agents taking object i to the "home" area. The attraction profile is

$$\sigma_i(\vec{D}_i) = A_\sigma \|\vec{D}_i - H\|^2 \tag{20}$$

A repulsion potential profile $R_{ij}(\vec{D}_{ij})$ from object j to object i is defined to make agents keep objects away from each other, which is expressed as

$$\lim_{\|\vec{D}_i - \vec{D}_j\|\to 0} \nabla_{\vec{D}_i - \vec{D}_j} R_{ij}(\|\vec{D}_i - \vec{D}_j\|) = R_{\max}, \quad \lim_{\|\vec{D}_i - \vec{D}_j\|\to \infty} \nabla_{\vec{D}_i - \vec{D}_j} R_{ij}(\|\vec{D}_i - \vec{D}_j\|) = 0 \tag{21}$$

Obviously, the repulsion force has the maximum value of $R_{\max}$.

The artificial potential energy of object i is $E_i = \sigma(\|\vec{D}_i\|) + \frac{1}{2}\sum_{j=1,j\neq i}^{M} R_{ij}(\|\vec{D}_i - \vec{D}_j\|)$. The strategy of velocity of transportation is to minimize the potential energy of objects. So the transportation velocity is of the form

$$\bar{v}_i = -\nabla_{\vec{D}_i} E_i = -\left(\nabla_{D_i}\sigma_i(\|\vec{D}_i\|) + \sum_{j=1,j\neq i}^{M} \nabla_{\vec{D}_i} R_{ij}(\|\vec{D}_i - \vec{D}_j\|)\right) \tag{22}$$

III.2.2. Stability of the system. Taking the total potential energies of objects as a Lyapunov function

$$V = \sum_{i=1}^{M} E_i = \sum_{i=1}^{M} \sigma_i(\|\vec{D}_i\|) + \frac{1}{2}\sum_{i=1}^{M}\sum_{j=1,j\neq i}^{M} R_i(\|\vec{D}_i - \vec{D}_j\|) \tag{23}$$

Then

$$\begin{aligned}
\dot{V} &= \sum_{i=1}^{M} \dot{\vec{D}}_i^T \nabla_{\vec{D}_i}\sigma(\|\vec{D}_i\|) + \frac{1}{2}\sum_{i=1}^{M}\sum_{j=1,j\neq i}^{M}\left(\dot{\vec{D}}_i^T - \dot{\vec{D}}_j^T\right) \times \left(\nabla_{(\vec{D}_i - \vec{D}_j)} R_{ij}(\|\vec{D}_i - \vec{D}_j\|)\right) \\
&= \sum_{i=1}^{M} \dot{\vec{D}}_i^T \nabla_{\vec{D}_i}\sigma(\|\vec{D}_i\|) + \sum_{i=1}^{M}\sum_{j=1,j\neq i}^{M} \dot{\vec{D}}_i^T \nabla_{\vec{D}_i} R_{ij}(\|\vec{D}_i - \vec{D}_j\|) \\
&= \sum_{i=1}^{M} \bar{v}_i^T \cdot X_{i3}\left(\nabla_{\vec{D}_i}\sigma(\|\vec{D}_i\|) + \sum_{j=1,j\neq i}^{M} \nabla_{\vec{D}_i} R_{ij}(\|\vec{D}_i - \vec{D}_j\|)\right) \\
&= \sum_{i=1}^{M}\left(-\left\|\nabla_{\vec{D}_i}\sigma(\|\vec{D}_i - H\|) + \sum_{j=1,j\neq i}^{M} \nabla_{\vec{D}_i} R_{ij}(\|\vec{D}_i - \vec{D}_j\|)\right\|^2 \cdot X_{i3}\right) \le 0.
\end{aligned} \tag{24}$$

When the system reaches the steady state, there are no objects at the center point of the "home" area, from (18), it holds that $\forall f_{i1} \neq 0$ $(i = 1, 2, \ldots, M)$. According to conclusion 1) in subsection III.I, it follows that $\lim_{t\to\infty} X_{i3} \neq 0$. According to the LaSalle principle, it is concluded that the system will converge to the minimization of the potential energies of objects, where $\bar{v}_i = 0$.

Remark 1: If $\lim_{t\to\infty} X_{i3} \neq 0$, in the steady state it holds that

$$\nabla_{\vec{D}_i}\sigma(\|\vec{D}_i - H\|) + \sum_{j=1,j\neq i}^{M} \nabla_{\vec{D}_i} R_{ij}(\|\vec{D}_i - \vec{D}_j\|) = 0, \quad (i = 1, 2, \ldots, M) \tag{25}$$

Adding up equations for all objects, because $\sum_{i=1}^{M}\sum_{j=1,j\neq i}^{M} \nabla_{\vec{D}_i} R_{ij}(\|\vec{D}_i - \vec{D}_j\|) = 0$, we obtain $\sum_{i=1}^{M} \nabla_{\vec{D}_i}\sigma(\|\vec{D}_i - H\|) = 0$. If let $\bar{D}$ represent the geometry center of all objects, we have

$$\begin{aligned}
\bar{D} - H &= \frac{1}{M}\sum_{i=1}^{M}(\vec{D}_i - H) \\
&= \frac{1}{A_\sigma M}\sum_{i=1}^{M} \nabla_{\vec{D}_i}\sigma(\|\vec{D}_i - H\|) = 0
\end{aligned} \tag{26}$$

It means that objects will be transported finally to the vicinity of the center of the "home" area. If define the position

https://doi.org/10.1017/S0263574705002195 Published online by Cambridge University Press

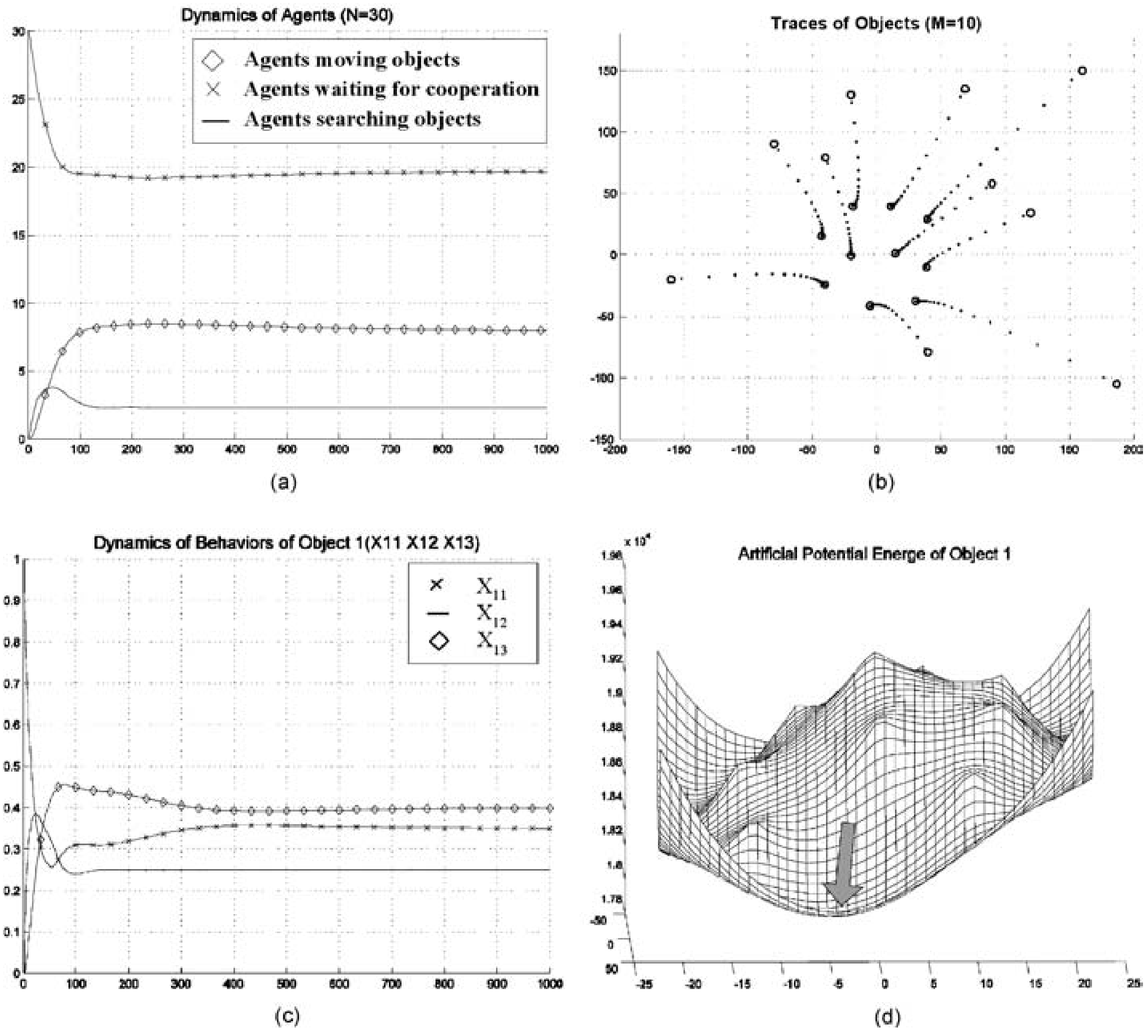

Fig. 2. Simulation result for the model with objects avoidance.

error for object i as $e_i = \vec{D}_i - H$, a Lyapunov function is defined as $V_i = \frac{1}{2}e_i^2$, then

$$\dot{V}_i = (\vec{D}_i - H)^T \left(-\nabla_{D_i}\sigma_i(\|\vec{D}_i - H\|) + \sum_{j=1, j\neq i}^{M} \nabla_{\vec{D}_i} R_{ij}(\|\vec{D}_i - \vec{D}_j\|) \right) \cdot X_{i3} \quad (27)$$

$$\leq \|\vec{D}_i - H\|[-A_\sigma\|\vec{D}_i - H\| + (M-1)\cdot R_{\max}]\cdot X_{i3} \quad (28)$$

Consequently, if $A_\sigma\|\vec{D}_i - H\| > R_{\max}(M-1)$, object i will be moved to the "home" area. Based on the analysis, it is concluded that if no object reaches the center of the "home" area, the expectant traces of the objects will converge to the "home" area. And, finally, all objects are distributed within a circular region with radius of $R_{\max}(M-1)/A_\sigma$ around the center of the "home" area.

Figure 2 shows the simulation results for the model. In simulation, there is a rectangle arena in which the center of the "home" area is at the origin (0, 0). Attachment and abandonment rates are of the forms $f_{i1}(\|\vec{D}_i - H\|) = \|\vec{D}_i - H\|/(K_a + \|\vec{D}_i - H\|)$ and $f_{i2}(\|\vec{D}_i - H\|) = K_g/(K_g + \|\vec{D}_i - H\|)$, respectively, where K_a, K_g are positive constants.

Figure 2 (a) to (d) show the dynamics of the agents numbers in different behaviors, the expectant moving traces of objects, the dynamics of states of object 1, and the artificial potential map for object 1 in the end. All objects are finally, distributed around the center of the "home" area, just like Fig. 2(b) shows. In Fig. 2(c), the line marked by diamonds represents the dynamics of the transportation state X_{13}. Because object 1 cannot reach the center of the home area, object 1 always has opportunity to be picked up by agents. Therefore X_{13} converges to a nonzero constant. But when object 1 reaches the lowest energy point in artificial potential field, which is indicated by an arrow in Fig. 2(d), the transportation velocity is zero. Therefore even object 1 has opportunity to be picked up by two agents, it can not be moved. Hence in the end, there always exists a part of swarms attaching to objects, but not moving them. It explains why the number of agents in the transportation behavior N_T, represented by the line marked by diamonds in Fig. 2(a), does not converge to zero.

If there is an object on the center of "home" area, equation (26) cannot hold consequentially. That means the expectant

https://doi.org/10.1017/S0263574705002195 Published online by Cambridge University Press

traces of objects do not converge to the center of the "home" area. In following section, we provide a modified design of swarm to overcome such disadvantage.

III.3. The model with bounded perceiving ability

This subsection provides a design of the swarm with higher performance than the one described above.

III.3.1. Improvements of the design of swarm. The swarm design and the mathematical model are improved in the following aspects:

1) The design in section III.2 only considers the avoidance between objects. But when objects are being moved, they may be blocked by other agents. Instead of taking objects away from blocking agents using artificial potential technique, abandoning transportation is more simple and practical. After the blocking agents leave, other agents will transport objects. Consequently, the model needs adding an encounter probability $\tilde{\alpha}$, which describes the probability at which an agent encounters an object in the transportation state. Hence the density of transition matrix is modified as

$$A_i = \begin{bmatrix} -\alpha N_S f_{i1} & \alpha N_{S(-\tau)}\Gamma_i & f_{i2} + \tilde{\alpha} N_S \\ \alpha N_S f_{i1} & -(\alpha N_{S(-\tau)}\Gamma_i + \alpha N_S f_{i1}) & 0 \\ 0 & \alpha N_S f_{i1} & -f_{i2} - \tilde{\alpha} N_S \end{bmatrix} \tag{29}$$

2) In practical applications, it's more convenient that all members adopt a constant transportation speed. Therefore the transportation velocity is modified whose expression will be proposed later. Consequently, attachment/abandonment rates need to be modified as

$$\lim_{\|E_i\|\to 0} f_{i1}\left(\left\|\nabla_{\vec{D}_i} E_i\right\|\right) = 0, \qquad \lim_{\|E_i\|\to\infty} f_{i1}\left(\left\|\nabla_{\vec{D}_i} E_i\right\|\right) = 1. \tag{30}$$

$$\lim_{\|E_i\|\to 0} f_{i2}\left(\left\|\nabla_{\vec{D}_i} E_i\right\|\right) = 1, \qquad \lim_{\|E_i\|\to\infty} f_{i2}\left(\left\|\nabla_{\vec{D}_i} E_i\right\|\right) = 0. \tag{31}$$

3) In practice, agents are subjected to sensing constraints, so that objects beyond the sensor bound cannot be sensed by agents. For the dynamics of agents' states, this constraint just affects the value of the perceiving ability α. But the constraint induces a non-smooth repulsion profile, which affects spatial dynamics of objects greatly. Figure 3 shows an example of the repulsion potential energy between two objects, where D_0 represents the sensing constraint of agents denoted by a vertical dashed line. Obviously, the modified repulsion profile is almost smooth anywhere in terms of $\|\vec{D}_i - \vec{D}_j\| = D_0$. And the profile satisfies the Lipschitz condition everywhere, which is expressed as

$$U_{ij}(\|\vec{D}_{ij}\|) = \begin{cases} R_{ij}(\|\vec{D}_i - \vec{D}_j\|), & \|\vec{D}_i - \vec{D}_j\| < D_0 \\ R_{ij}(D_0), & \|\vec{D}_i - \vec{D}_j\| \geq D_0 \end{cases} \tag{32}$$

where $R_{ij}(\|\vec{D}_i - \vec{D}_j\|)$ is a smooth repulsion profile that obeys principles in (21).

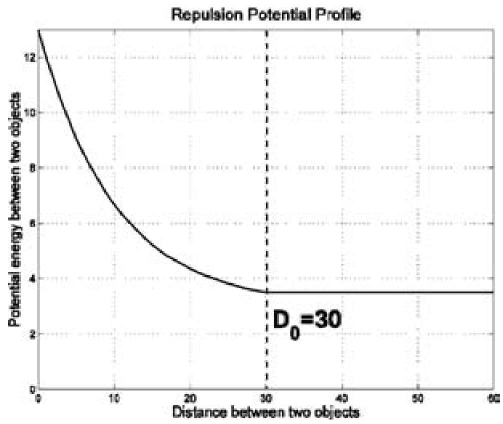

Fig. 3. The repulsive potential profile of object i.

III.3.2. New transportation velocity. The artificial potential energy function of object i is

$$E_i(\|\vec{D}_i\|) = \sigma(\|\vec{D}_i - H\|) + \frac{1}{2}\sum_{j=1, j\neq i}^{M} U_{ij}(\|\vec{D}_{ij}\|) \tag{33}$$

where $\sigma(\|\vec{D}_i - H\|)$ is of the form in (20), $U_{ij}(\|\vec{D}_{ij}\|)$ represents the repulsion potential profile which is designed as

$$U_{ij}(\|\vec{D}_{ij}\|) = \begin{cases} R_{\max}\cdot B\cdot \mathrm{EXP}(-\|\vec{D}_{ij}\|/B), & \|\vec{D}_{ij}\| < D_0 \\ R_{\max}\cdot B\cdot \mathrm{EXP}(-D_0/B), & \|\vec{D}_{ij}\| \geq D_0 \end{cases} \tag{34}$$

where B is a positive constant.

The strategy of the transportation velocity is still to minimize total potential energy of object. Therefore we should find the expression of $\nabla_{\vec{D}_i} E_i$.

Firstly, we consider a repulsive potential profile. To simplify the notation, we drop the subscripts ij. The generalized directional derivative[19] of U at the point $\|\vec{D}\| = D_0$ in an arbitrary direction v is calculated as follows.

If $v > 0$, it holds that $U(y + tv) - U(y) \leq 0$. Then it follows that $\sup_{y\in\delta(D_0)}(U(y+tv) - U(y)) = 0$, where $\delta(D_0)$ is a closure region around $\|D\| = D_0$. We obtain

$$U^\circ(D_0; v) = \limsup_{\substack{y\to D_0 \\ t\downarrow 0}} \frac{U(y+tv) - U(y)}{t} = 0 \tag{35}$$

If $v < 0$,

$$\begin{aligned} U^\circ(D_0; v) &= \limsup_{\substack{y\to D_0 \\ t\downarrow 0}} \frac{U(y+tv) - U(y)}{t} \\ &= \limsup_{\substack{y\to D_0 \\ t\downarrow 0}} \frac{R(y+tv) - R(D_0)}{t} \\ &= \lim_{t\downarrow 0} \frac{R(D_0+tv) - R(D_0)}{t} = c(v) > 0 \end{aligned} \tag{36}$$

where $c(v)$ is a linear function of v. On the other hand, the classical derivative on point $\|\vec{D}\| = D_0$ in direction of v is calculated as follows.

$$\text{If } v > 0,\ U'(D_0; v) = \lim_{t\downarrow 0}[(R(D_0) - R(D_0))/t] = 0.$$
$$\text{If } v < 0,\ U'(D_0; v) = \lim_{t\downarrow 0}[(R(D_0 + tv) - R(D_0))/t] = c(v).$$

Consequently, at point $\|\vec{D}\| = D_0$, $U'(\|\vec{D}\|; v) = U^\circ(\|\vec{D}\|; v)$. Due to the smooth property, at any point that $\|\vec{D}\| \neq D_0$, it is easily proved that $U'(\|\vec{D}\|; v) = U^\circ(\|\vec{D}\|; v)$. Thus the repulsion profile (32) is regular. Therefore the generalized gradient of U at $\|\vec{D}\|$ is the set given by $\partial U(\|\vec{D}\|) = \{\zeta : U^\circ(\|\vec{D}\|) \geq \langle \zeta, v\rangle$ for all v in $\Omega\}$, where Ω is a Banach space. And ζ denotes one linear function $\zeta : \Omega \to R$. For all $\|\vec{D}\| \neq D_0$, it holds that $\partial U(\|\vec{D}\|) = \nabla_{\vec{D}} U(\|\vec{D}\|)$. At the point $\|\vec{D}\| = D_0$, if repulsion profile is of the form in (33), it is easily proved that

$$\partial U(\|D_0\|) = [-R_{\max} \cdot EXP(-D_0/B),\quad 0] \tag{37}$$

Since the attractive potential profile $\sigma(\|\vec{D}_i\|)$ is a smooth function, it is regular too. The artificial potential energy function is a positive linear combination of functions of attraction and repulsion potential profiles. It also satisfies the Lipschitz condition. According to the chain rule I of general derivative,[19] we obtain the general derivative of the total potential energy as

$$\partial E_i = \overline{co}\left\{\partial\sigma(\|\vec{D}_{ij}\|) + \sum_{j=1, j\neq i}^{M} \zeta_{ij},\ \zeta_{ij} \in \partial U(\|\vec{D}_{ij}\|)\right\} \tag{38}$$

where $\overline{co}$ denotes weak-closed convex hull.

It is easily proved that

$$\partial_{\vec{D}_i} U(\|\vec{D}_{ij}\|) = \partial_{\vec{D}_{ij}} U(\|\vec{D}_{ij}\|) \cdot \frac{\partial\|\vec{D}_{ij}\|}{\partial \vec{D}_i} \tag{39}$$

Substituing it into (38), we can conclude $\nabla_{\vec{D}_i} E_i = \partial E_i (i = 1, 2, \ldots, M)$. Therefore according to the improvement 2), we define the transportation speed as

$$\bar{v}_i = \begin{cases} -S_t \cdot \dfrac{\nabla_{\vec{D}_i} E_i}{\|\nabla_{\vec{D}_i} E_i\|} = -S_t \dfrac{\partial E_i}{\|\partial E_i\|}, & \partial E_i \neq 0 \\ 0, & \partial E_i = 0 \end{cases} \tag{40}$$

where S_t is a positive constant.

III.3.3. Stability of the swarm. According to (11), the Filippov solution of the expectant moving speed of object i is

$$\dot{\vec{D}}_i \in K[f](\vec{D}_i) \tag{41}$$

where $K[f] \equiv \cap_{\delta>0} \cap_{\mu N=0} \overline{co} f(B(\vec{D}_i, \delta) - N)$, $f(y) = -S_t \frac{\partial_y E}{\|\partial_y E\|} \cdot X_y$, where $\cap_{\mu N=0}$ denotes the intersection over all set N of Lebesgue measure zero.

Applying the Lyapunov theorem for a non-smooth system, we define the Lyapunov function as $V = \sum_{i=1}^{M} E_i$, which is Lipchitz and regular. Then V is absolutely continuous, $\frac{d}{dt} V(\vec{D})$ exists almost everywhere and

$$\frac{d}{dt} V(\vec{D}) \overset{a.e}{\in} \dot{\tilde{V}}(\vec{D}) \tag{42}$$

where

$$\begin{aligned} \dot{\tilde{V}}(\vec{D}) &= \sum_{i=1}^{M} \dot{\tilde{V}}_i(\vec{D}_i) \\ &= \sum_{i=1}^{M} \bigcap_{\zeta_i \in \partial E(\vec{D}_i)} \zeta_i^T K[f](\vec{D}_i) \\ &= \sum_{i=1}^{M} \bigcap_{\zeta \in \partial E_i(\vec{D}_i)} -S_t \cdot \zeta_i^T \cdot \frac{\partial E_i}{\|\partial E_i\|} \cdot X_{i3} \end{aligned} \tag{43}$$

For object i in the transportation state, according to the definition of attraction/repulsion profile, it holds that $\partial\sigma(\|\vec{D}_{ij}\|) \geq 0$ and $\zeta_i \leq 0$, $\zeta_i \in \sum_{j=1, j\neq i}^{M} \partial U(\|\vec{D}_{ij}\|)$. Consider two situations:

1) At time t, $\forall j$, $j \neq i$, $\|\vec{D}_{ij}\| \neq D_0$. It holds that $\zeta_i = \nabla E_i$. Hence we have

$$\dot{\tilde{V}}_i(\vec{D}_i) = -S_t \nabla E_i^T \cdot \frac{\nabla E_i}{\|\nabla E_i\|} \cdot X_{i3} \leq 0 \tag{44}$$

Obviously, when $\nabla E_i = 0$, according to (30) and (31), $f_{i1} = 0$, $f_{i2} = 1$. Recalling conclusion 2) in section 3.1, we have $X_{i3} = 0$.

2) At time t, $\exists j$, $j \neq i$, $\|\vec{D}\| = D_0$. There are also two situations.

(i) In case of $0 \notin \partial E_i$, it is illustrated in Fig. 4.

Because all $\zeta_i \in \partial E_i$ have an identical sign, then

$$\bigcap_{\zeta_i \in \partial E_i} \zeta_i^T \cdot \partial E_i = \min(\|\zeta_i\|) \cdot \max(\|\zeta\|) > 0 \tag{45}$$

Substituting (45) into the Lyapunov function of object i, we obtain

$$\dot{\tilde{V}}_i(\vec{D}_i) = -S_t \cdot \bigcap_{\zeta_i \in \partial E_i} \min(\|\zeta_i\|) \cdot \max(\|\zeta_i\|) \cdot \frac{X_{i3}}{\|\partial E_i\|} < 0 \tag{46}$$

(ii) In case of $0 \in \partial E_i$, it is illustrated in Fig. 5.

There must exist $\zeta_i = 0$, $\zeta_i \in \partial E_i$. It follows that

$$\dot{\tilde{V}}_i(\vec{D}_i) = -\bigcap_{\zeta_i \in \partial E_i} S_t \zeta_i^T \cdot \frac{\partial E_i}{\|\partial E_i\|} \cdot X_{i3} = 0. \tag{47}$$

Different from the situation 1), here $X_{i3} \neq 0$.

Combining all situations, we have $\dot{\tilde{V}}_i(\vec{D}_i) \leq 0$. Substituting it into (43), we can obtain

$$\dot{\tilde{V}}(\vec{D}) = \sum_{i=1}^{M} \dot{\tilde{V}}_i(\vec{D}_i) \leq 0. \tag{48}$$

https://doi.org/10.1017/S0263574705002195 Published online by Cambridge University Press

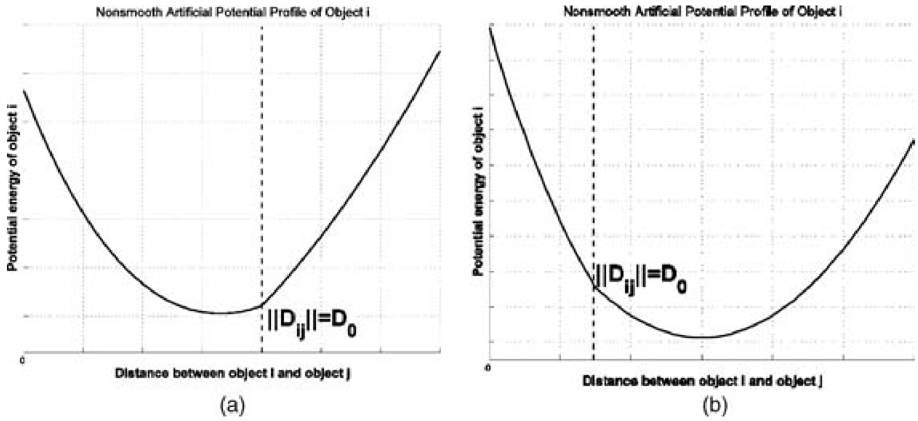

Fig. 4. The situation in case of $0 \notin \partial E_i$.

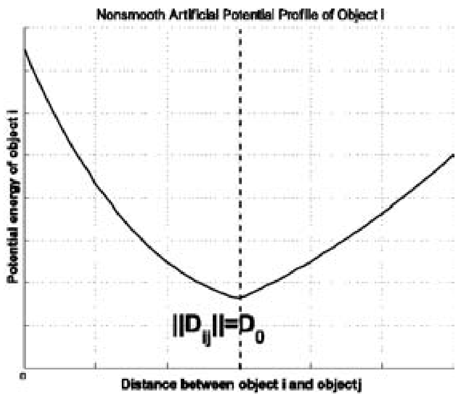

Fig. 5. The situation in case of $0 \in \partial E_i$.

According to LaSalle's principle of the Filippov solution, we draw the conclusion that the system must converge to the largest invariant set in the closure $\{\vec{D}_i \in \Omega | 0 \in \tilde{\dot{V}}\}$. At the equilibrium, $\tilde{\dot{V}}_i(\vec{D}_i) = 0$. Furthermore, the invariant set also equals $\{\vec{D}_i \in \Omega | 0 \in \partial E_i, i = 1, \ldots, M\}$.

Remark 2: According to (39), the resultant force of action/reaction between two objects i and $j (i \neq j)$ satisfies

$$F_{ij} = \partial_{\vec{D}_{ij}} U(\|\vec{D}_{ij}\|) + \partial_{\vec{D}_{ji}} U(\|\vec{D}_{ji}\|)$$
$$= \partial_{\vec{D}_j} U(\|\vec{D}_{ij}\|) - \partial_{\vec{D}_i} U(\|\vec{D}_{ij}\|) = 0. \qquad (49)$$

That means, even of the repulsion profile is non-smooth, the action/reaction principle of Newton theorems still holds. When the swarm reaches the invariant set, it holds that $0 \in \partial E_i (i = 1, 2, \ldots, M)$. Adding all ∂E_i and considering (49), we get $0 \in \sum_{i=1}^{M} \nabla_{\vec{D}_i} \sigma_i(\vec{D}_i)$. Because $\nabla_{\vec{D}_i} \sigma_i(\vec{D}_i)$ is a smooth function, we have $\sum_{i=1}^{M} \nabla_{\vec{D}_i} \sigma_i(\vec{D}_i) = 0$, which is the same as the result in **Remark 1**. So it is concluded that all objects are transported into the "home" area and distributed around the center of the "home" area in terms of $\frac{1}{M} \sum_{i=1}^{M} (\vec{D}_i - H) = 0$. Here there is no need to suppose that $\lim_{t \to \infty} X_{i3} \neq 0$.

Figure 6 shows the simulation results of the swarm. The arena is the same as the previous simulation one. And all figures are defined as the same as the previous simulation. In the simulation, attachment/abandonment rates are of the forms

$$f_{i1}\left(\left\|\nabla_{\vec{D}_i} E_i\right\|\right) = \frac{\left\|\nabla_{\vec{D}_i} E_i\right\|}{K_a + \left\|\nabla_{\vec{D}_i} E_i\right\|},$$

$$f_{i2}\left(\left\|\nabla_{\vec{D}_i} E_i\right\|\right) = \frac{K_g}{K_g + \left\|\nabla_{\vec{D}_i} E_i\right\|}.$$

From Fig. 6(b), we observe that the system also converges to the state where all objects are transported to their lowest potential energy points. For example, the position indicated by an arrow in Fig. 6(d) is the lowest energy point of object 1. According to **Remark 2**, all objects are finally distributed around the center of the "home" area. From the proof of the stability, we know that some objects maybe stabilize on nonsmooth equilibrium, where the probability of transportation state is not zero. For example, the dynamics of states of object 1 is shown in Fig. 6(c), in which the line representing the transportation state marked by diamond converges to a nonzero value. This means the lowest potential energy point of object 1 is a nonsmooth equilibrium. Consequently, N_T, the number of agents moving objects marked by the diamond in Fig. 6(a), also converges to a nonzero value.

Remark 3: Because of the improvement 1), the stationary distribution of object i's transportation state should be rewritten as

$$\pi_{i3} = \frac{\alpha N_S f_{i1}^2}{\alpha N_S f_{i1}^2 + (f_{i2} + \tilde{\alpha} N_S)(2 f_{i1} + \Gamma_i)} \qquad (50)$$

From the dynamics of agents in Fig. 6(a) and dynamics of states of object 1 in Fig. 6(c), during a period of Ψ that is shortly after the beginning and before 400 iterations, it is observed that, i) dynamics of agents' states and objects' states are relatively trivial. We think that the distribution of objects' states approximates a stationary distribution where it holds that $X_{i3}(t) \approx \pi_{i3}$, $t \in \Psi$; ii) for object 1, the value of $X_{13}(t)$ is higher than it is during other period. According to (11), if the transportation velocity is fixed, the expectant moving speed of object is determined by $X_{i3}(t)$. Hence the expectant moving speed of object during period of Ψ determines how fast the object is transported to the "home" area.

https://doi.org/10.1017/S0263574705002195 Published online by Cambridge University Press

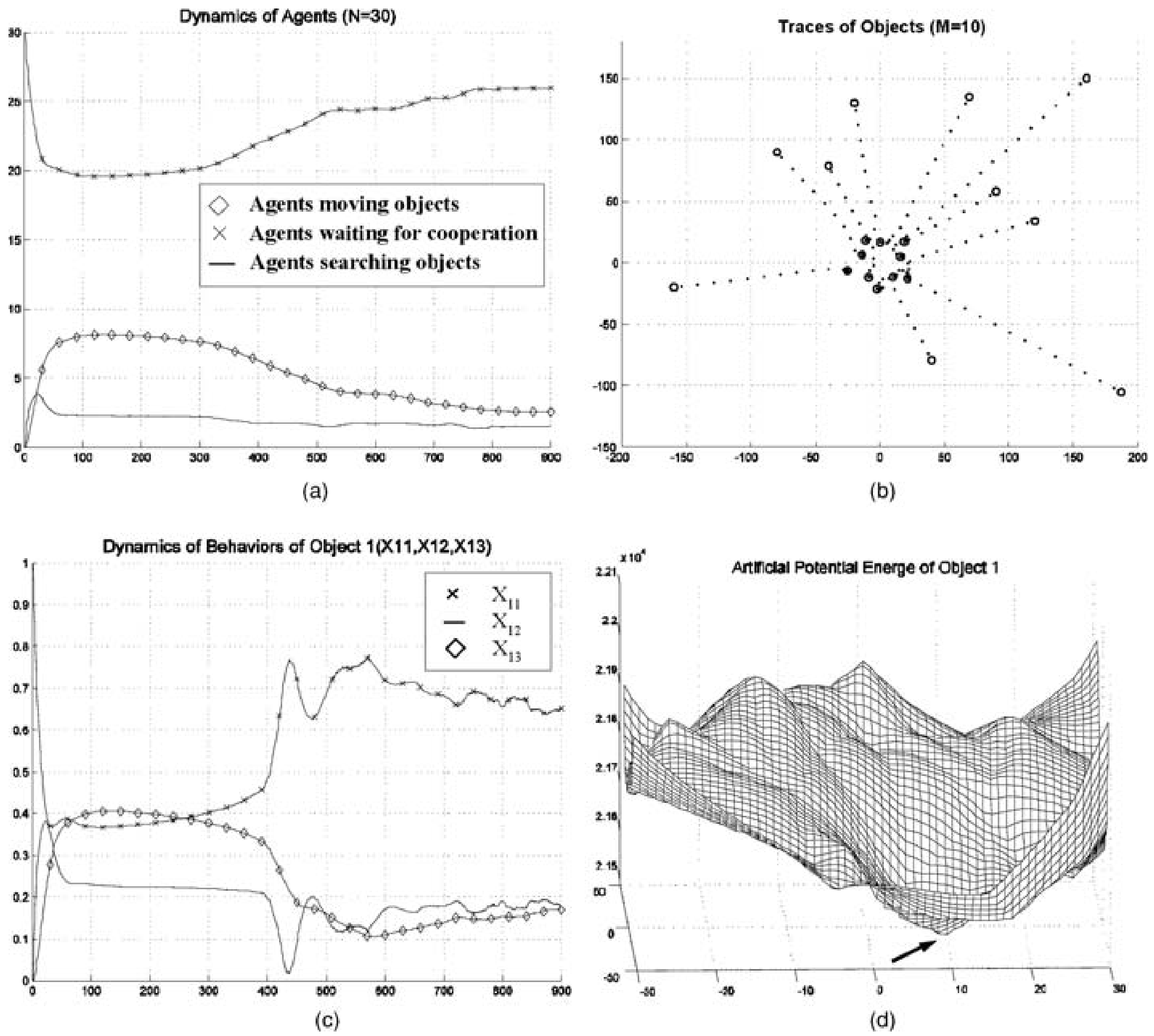

Fig. 6. Simulation results of the model with sensor constraints.

Based on (50), we can analyze what and how parameters affect $X_{i3}(t)\,(t \in \Psi)$. If the number of agents increases, N_S increases. And from (3), we know that the longer the period of τ is, the higher N_S and the smaller Γ_i is. Consequently, X_{i3} in Ψ can be improved by increasing the size of the swarm N and enlarging waiting period τ.

However, there is a limit of X_{i3} when N_S increases.

$$\lim_{N_S \to \infty} X_{i3}(t) = \lim_{N_S \to \infty} \pi_{i3} \approx \frac{\alpha f_{i1}}{\alpha f_{i1} + 2\tilde{\alpha}} \tag{51}$$

where $t \in \Psi$, i. e. when the size of a swarm is very large, increasing the number of agents will make little sense for improving performance. And the upper limit of the probability of the transportation state is determined by f_{i1}, α, and $\tilde{\alpha}$. Since α, and $\tilde{\alpha}$ are determined by the physical properties of agent; the crucial way to speed collecting is to design a proper attachment strategy so that agents have much interest to move objects outside the "home" area.

IV. CONCLUSIONS

The cooperative collecting task performed by autonomous mobile robots can be realized by swarms, and a technique is presented for modeling multi-behavior swarms. The model includes two levels, a high level describing dynamics of behavior change using a macroscopic model based on the Markov process, and a low level describing expectant individual movements in the behaviors that we are interested in. Individual movements in certain behaviors are described as an individual-based (Lagrangian) model based on an artificial potential profile. The mathematical proofs and simulations show that the design of a swarm system for collecting task is valid. Because the dynamics of behaviors is a kind of dynamics of expectant distribution, the model cannot describe an actual spatio-temporal trajectory of a swarm, but it reveals a statistical expectant of swarm.

It is only in the transportation state that there needs an explicit communication between two cooperative agents for coordinating their moving speed. And communication costs in swarms having different size are almost the same. Therefore a swarm can be expanded to a large scale without increasing communication cost.

Acknowledgements

The authors appreciate the fund support from the research committee of University of Macau under grant no. RG082/04-05S/LYM/FST.

References

1. G. Beni and J. Wang, "Swarm intelligence", *The 7th Annual Meeting of the Robotics Society of Japan*, Tokyo, Japan (1989) pp. 425–428.
2. S. Hackwood and G. Beni, "Self-organization sensors by deterministic annealing", *IEEE/RSJ International Conference on Intelligent Robot and Systems*, Los Alamitos, CA (1991) pp. 1177–1183.
3. A. Martinoli and K. Easton, "Modeling swarm robotic system", *The 8th International Symposium on Experimental Robotics,* Sant'Angelo d'Ischia, Italy (2002) pp. 297–306.
4. K. Lerman, A. Galstyan, A. Martinoli and A. J. Ijspeert, "A macroscopic analytical model of collaboration in distributed robotic systems", *Artificial Life* **7**(4), 375–393 (2001).
5. A. Mogilner and L. Edelstein-Keshet, "A nonlocal model for a swarm", *Journal of Mathematical Biology* **38**, 534–570 (1999).
6. L. Edelstein-Keshet, "Mathematical models of swarming and social aggregation", *The 2001 International Symposium on Nonlinear Theory and its Applications*, Miyagi, Japan (2001) pp. 1–7.
7. V. Gazi and K. M. Passion, "Stability analysis of social foraging swarms", *IEEE Transaction on System, Man, and Cybernetics-Part B: Cybernetics* **34**(1), 539–557 (2004).
8. J. R. T. Lawton, R. W. Beard and B. J. Young, "A decentralized approach to formation maneuvers", *IEEE Transactions on Robotics and Automation* **19**(6), 933–941 (2003).
9. H. G. Tanner, A. Jadbabaie and G. J. Pappas, "Stable flocking of mobile agents, part I: fixed topology", *The 42nd IEEE Conference on Decision and Control*, Hyatt Regency Maui, Hawaii, USA (2003) **Vol. 2**, pp. 2010–2015.
10. Y. Liu, K. M. Passino, and M. Polycarpou, "Stability analysis of m-dimensional asynchronous swarms with a fixed communication topology", *IEEE Transactions on Automatic Control* **48**(1), 76–95 (2003).
11. V. Gazi and K. M. Passino, "Stability analysis of swarm", *IEEE Transactions on Automatic Control* **48**(4), 692–697 (2003).
12. J. H. Reif and H. Wang, "Social potential fields: a distributed behavioral control for autonomous robots", *Robotics and Autonomous Systems* **27**(3) 171–194 (1999).
13. N. E. Leonard and E. Fiorelli, "Virtual leaders, artificial potentials and coordinated control of groups", *The 40th IEEE Conference on Decision and Control*, Orlando, FL, USA (2001) pp. 2968–2973.
14. A. Mogilner, L. Edelstein-Keshet, L. Bent and A. Spiros, "Mutual interactions, potentials, and individual distance in a social aggregation", *Journal of Mathematical Biology*. **47**, 353–389 (2003).
15. Y. Li and X. Chen, "Control and stability analysis on multiple robots formation", *The 2th International Conference on Autonomous Robots and Agents*, New Zealand (2004) pp. 158–163.
16. Y. Li and X. Chen, "Modeling and simulation of a swarm of robots for box-pushing task", *The 12th Mediterranean Conference on Control and Automation*, Kusadasi, Izmir, Turkey (June, 2004) (CD-ROM).
17. Y. Li and X. Chen, "Mathematical analysis on a swarm of robotic system", *The 1st Asia International Symposium on Mechatronics*, Xian, China (Sep. 2004) pp. 653–658.
18. Y. Li and X. Chen, "Formation Control for a Multiple Robotic System Using Adaptive Neural Network", *Advances in Neural Networks* (Eds. by J. Wang, X. Liao and Z. Yi) (Springer, LNCS 3498, Part III, 2005), pp. 228–233.
19. F. H. Clarke, *Optimization and Nonsmooth Analysis*. (Classics in applied mathematics 5, SIAM, 1990).